

PAPER • OPEN ACCESS

On Impact Problems Of Projectile Using Meshless Peridynamics Analysis

To cite this article: Mas Irfan P. Hidayat 2019 *IOP Conf. Ser.: Mater. Sci. Eng.* **547** 012019

View the [article online](#) for updates and enhancements.



IOP | ebooks™

Bringing you innovative digital publishing with leading voices to create your essential collection of books in STEM research.

Start exploring the collection - download the first chapter of every title for free.

On Impact Problems Of Projectile Using Meshless Peridynamics Analysis

Mas Irfan P. Hidayat^{1*}

¹Department of Materials and Metallurgical Engineering-FTI, Institut Teknologi Sepuluh Nopember, Kampus ITS Keputih Sukolilo 60111, Surabaya

*E-mail: irfan@mat-eng.its.ac.id

Abstract. In this study, impact problems of projectile are investigated using meshless peridynamics analysis. Two impact cases of rigid projectiles having different stiffness values against aluminum target are examined numerically. The problems are simulated in LAMMPS software environments. For each case, numerical parameters affecting perforation patterns of target body are discussed in detail. This work focuses on the effects of numerical parameters of indenter stiffness (k) and critical bond stretch parameter alpha on the perforation patterns of the target for various impact velocities. Numerical results show that larger perforation is produced with the increase of k value of indenter. In addition, it is observed that the impacted plate appears to be more deflected, if greater value of α is employed.

Keywords: impact, projectile, peridynamics, LAMMPS

1. Introduction

Fracture of solids is main concern in engineering and industrial applications. Such material failure is important because integrity of a structure or component during its service is affected by the event of failure [1-3]. Amongst modes of failure is fracture due to impact, which is mainly characterized by collision particularly with an indenter of high speed. From numerical viewpoint, simulation of fracture is a challenging task. This is due to the fact that the initiation site/time of failure and failure direction in a material need to be determined accurately. On the other hand, how to realistically and efficiently simulate the material failure is difficult as well. In finite element (FE), process of re-meshing is frequently needed to adapt with new configuration of structure due to the failure. Obviously, the task would be cumbersome and time consuming [4]. Recently, a class of numerical techniques called as meshfree methods is intensively pursued for efficient modeling of fracture of materials [5-8].

In this study, impact problems of projectile are investigated using meshless peridynamics analysis. Two impact cases of rigid projectiles having different stiffness values against aluminum target are examined numerically. The problems are simulated in LAMMPS [9]. For each case, numerical parameters affecting perforation patterns of target body are discussed in detail. This work focuses on the effects of numerical parameters of indenter stiffness (k) and critical bond stretch parameter (α) on the perforation patterns of the target.



2. Materials and Methods

In classical continuum mechanics, differential notion is extensively used to represent equilibrium condition of media under the influence of forces/displacements exerted to it. Peridynamics is a reformulation of the classical continuum mechanics equations having a distinct advantage in treating discontinuities in solids. By employing non-local interaction concept, peridynamics resorts to formulation based upon integration rather than differentiation. As a result, it can naturally handle fracture events without necessity to use deformation gradients [10-13].

$$\rho(\mathbf{x})\ddot{\mathbf{u}}(\mathbf{x},t) = \int_{H_x} \mathbf{f}(\hat{\mathbf{u}}(\mathbf{x},t) - \mathbf{u}(\mathbf{x},t), \hat{\mathbf{x}} - \mathbf{x}) dV_x + \mathbf{b}(\mathbf{x},t) \quad \text{for } \mathbf{x} \in \Omega \quad \text{and } t \in [t_0, \infty] \quad (1)$$

where: Ω is the problem domain, ρ is material density, \mathbf{f} is the pairwise force function in peridynamic bond connecting material points $\hat{\mathbf{x}}$ and \mathbf{x} , \mathbf{u} and $\ddot{\mathbf{u}}$ are the displacement and acceleration vector, respectively, \mathbf{b} is the body force, t and t_0 are time and initial time, respectively, H_x is horizon region, a local region in which the integral is defined. In addition, δ is defined as radius of the region, commonly taken as circle/disk in 2D or sphere in 3D.

Furthermore, a pairwise potential ϕ exists for a microelastic material such that:

$$\mathbf{f}(\xi, \boldsymbol{\eta}) = \frac{\partial \phi(\xi, \boldsymbol{\eta})}{\partial \boldsymbol{\eta}} \quad (2)$$

where: $\xi = \hat{\mathbf{x}} - \mathbf{x}$ is the relative position and $\boldsymbol{\eta} = \mathbf{u}(\hat{\mathbf{x}}, t) - \mathbf{u}(\mathbf{x}, t)$ is the relative displacement.

The micropotential is defined as:

$$\phi(\xi, \boldsymbol{\eta}) = \frac{1}{2} c s^2 \|\xi\| \quad (3)$$

$$s = \frac{\|\boldsymbol{\eta} - \xi\| - \|\xi\|}{\|\xi\|} \quad (4)$$

where: c constant and s bond stretch or strain.

Noting that with K the bulk modulus and δ the horizon, c for 3D models is given by:

$$c = \frac{18K}{\pi\delta^4} \quad (5)$$

Damage is defined as breakage of material bonds. For a prototype microelastic brittle (PMB) material, the pairwise function is given by:

$$\mathbf{f}(\xi, \boldsymbol{\eta}) = g(\xi, \boldsymbol{\eta}) \frac{\boldsymbol{\eta} + \xi}{\|\boldsymbol{\eta} + \xi\|} \quad (6a)$$

$$g(\xi, \boldsymbol{\eta}) = \begin{cases} cs(t, \xi, \boldsymbol{\eta}) \mu(\xi, \boldsymbol{\eta}), & \|\xi\| \leq \delta \\ 0 & \|\xi\| > \delta \end{cases} \quad (6b)$$

$$\mu(\xi, \boldsymbol{\eta}) = \begin{cases} 1 & \text{if } s(t, \xi, \boldsymbol{\eta}) < \min(s_0(t, \xi, \boldsymbol{\eta}), s_0(t, \xi', \boldsymbol{\eta}')) \text{ for all } 0 \leq t' \leq t \\ 0 & \text{otherwise} \end{cases} \quad (7)$$

where: μ is the history-dependent scalar boolean function. $s_0(t, \xi, \boldsymbol{\eta})$ is a critical stretch, determined by parameters of critical bond stretch s_{00} and α , such that:

$$s_0(t, \xi, \boldsymbol{\eta}) = s_{00} - \alpha s_{\min}(t, \xi, \boldsymbol{\eta}), \quad s_{\min}(t) = \min_{\xi} s(t, \xi, \boldsymbol{\eta}) \quad (8)$$

3. Results and Discussion

Aluminum cylindrical plate impacted by a rigid sphere indenter is considered in this study. The indenter is located at 0.0051 m from the plate and its velocity is varied from 200 to 400 m/s. Material properties for the aluminum plate are given in Table 1 below. For plotting the simulation results, OVITO [14] and MATLAB [15] soft-wares are employed.

Table 1. Properties of aluminum plate and parameters of simulation

Properties/parameters	Values
Density (ρ)	2700 kg/m ³
Bulk modulus (K)	69E9 Pa
Poisson ratio (ν)	0.33
Fracture toughness (K_{Ic})	24 MPa√m
Horizon (δ)	0.0015
Critical bond stretch parameter 1 (s_{00})	0.00627
Critical bond stretch parameter 2 (α)	0.0 and 0.25
Indenter stiffness k	1E17 and 1E12
Time step	1E-7 sec

3.1. Influence of parameter k

Simulation results of perforation patterns on the plate are presented in Fig. 1. The stiffness value k is set to be 1E17, and two α values as given in Table 1 are employed.

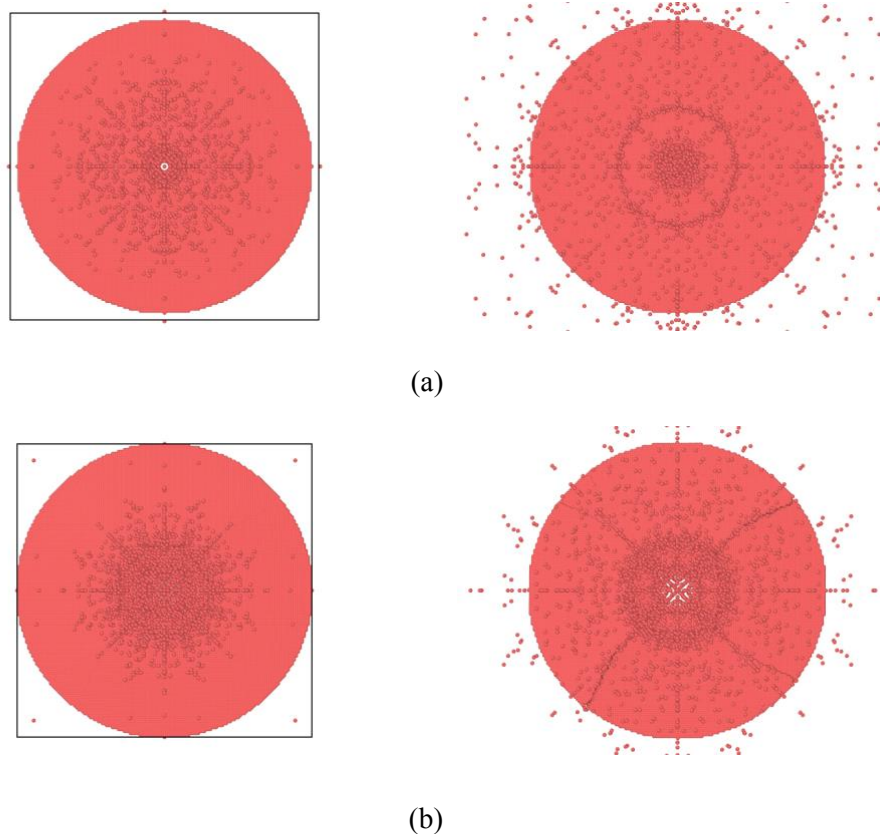


Fig. 1. Perforation patterns on the plate with: (a) $\alpha = 0$, and (b) $\alpha = 0.25$, taken at simulation steps of 1000 and 1800, respectively (velocity = 300 m/s and $k = 1E17$).

Fig. 2 shows the results of perforation patterns on the plate with the stiffness value k is set to be 1E20. Hence, the current indenter is harder than the previous one. From the results, it is seen that greater k value gives larger impact and perforation, for the same impact velocity.

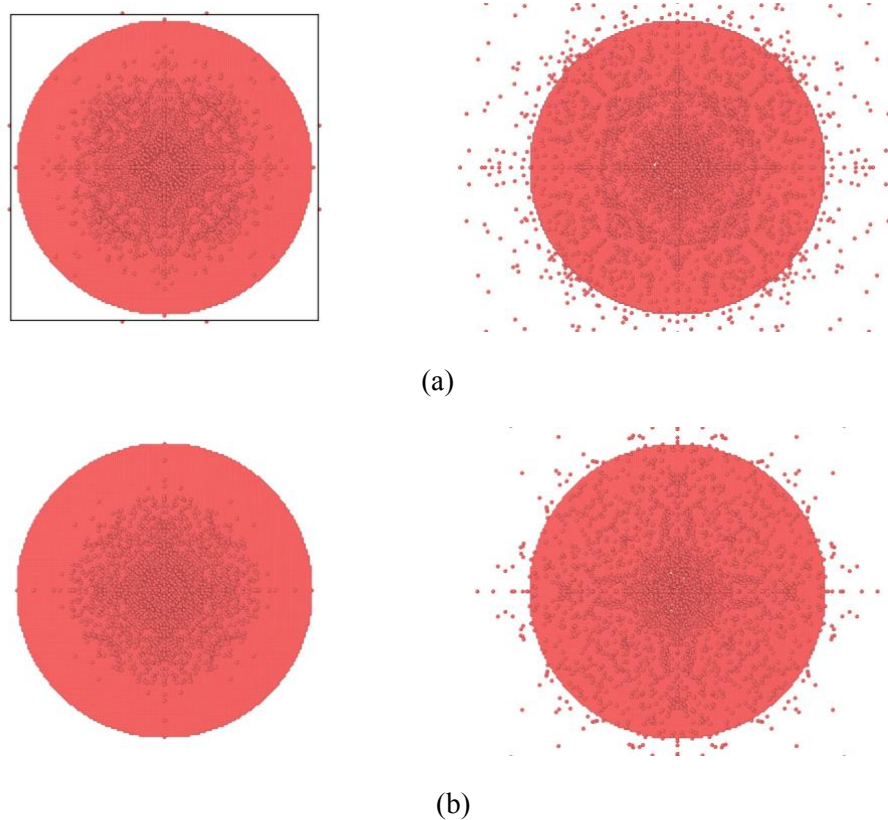


Fig. 2. Perforation patterns on the plate with: (a) $\alpha = 0$, and (b) $\alpha = 0.25$, taken at simulation steps of 1000 and 1800, respectively (velocity = 300 m/s and $k = 1E20$).

In addition, development of pressure during the simulation steps for various values of velocities and α is shown in Fig. 3. Note that the results are consistent with respect to the increase of k value.

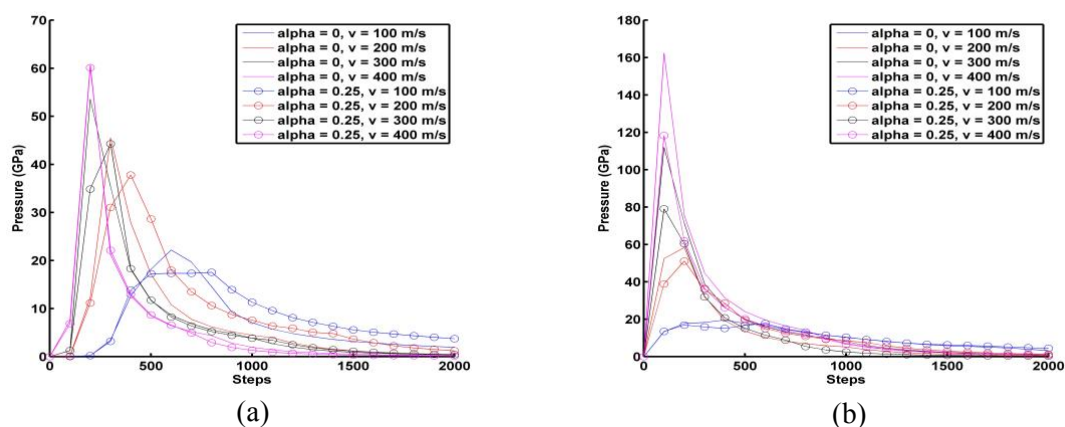


Fig. 3. Pressure during time steps for various impact velocities and α values with: (a) $k = 1E17$, and (b) $k = 1E20$.

3.2. Debris development

Development of debris from step to step is presented as well here, as shown in Figs. 4-7. The obtained results consistently show that greater debris development is obtained with the increase of indenter stiffness value. Moreover, more interesting discussion may be casted concerning with the influence of parameter α to perforation development, as in the following section.

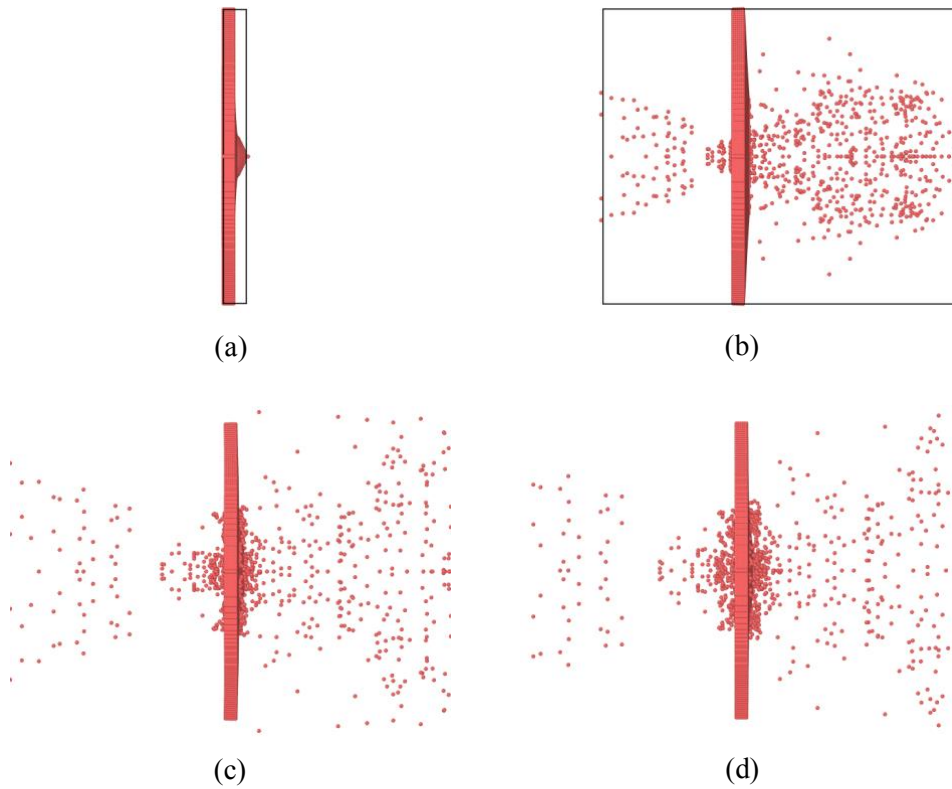


Fig. 4. Debris development at several simulation steps: (a) 200, (b) 800, (c) 1400, and (d) 1600 (the impact velocity = 300 m/s, $\alpha = 0$, $k = 1E17$).

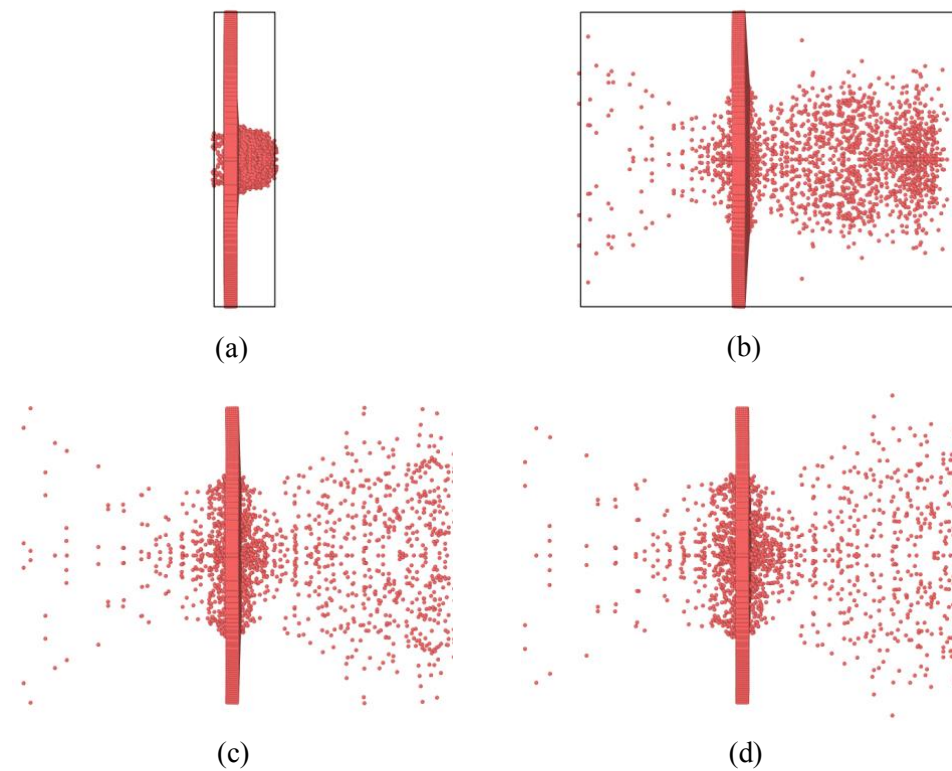


Fig. 5. Debris development at several simulation steps: (a) 200, (b) 800, (c) 1400, and (d) 1600 (velocity = 300 m/s, $\alpha = 0$, $k = 1E20$).

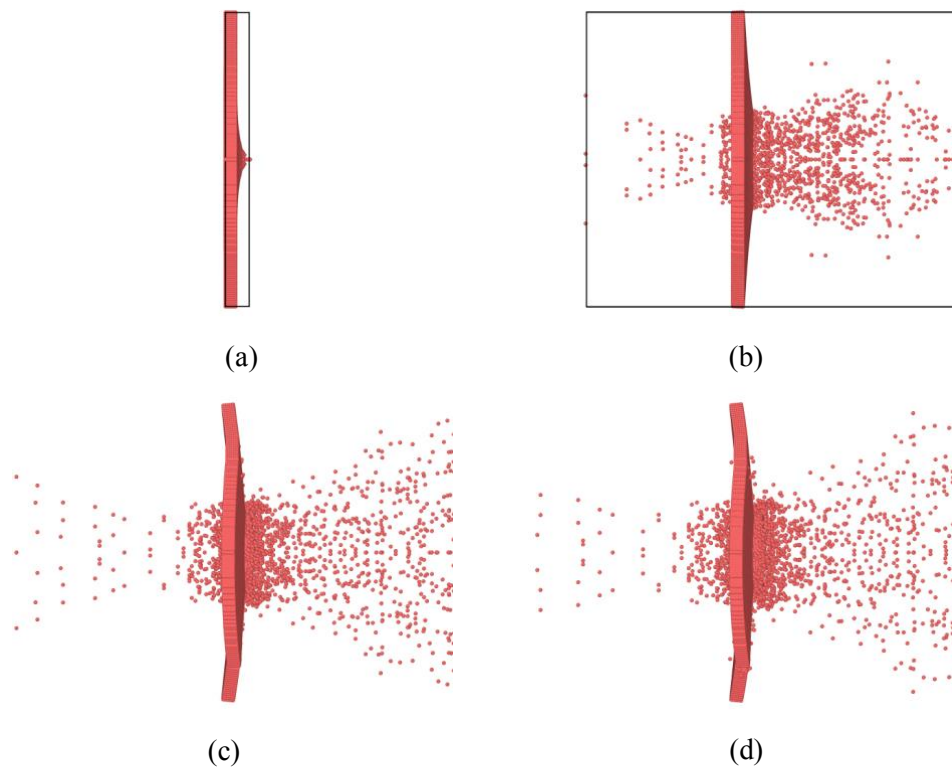


Fig. 6. Debris development at several simulation steps: (a) 200, (b) 800, (c) 1400, and (d) 1600 (the impact velocity = 300 m/s, $\alpha = 0.25$, $k = 1E17$).

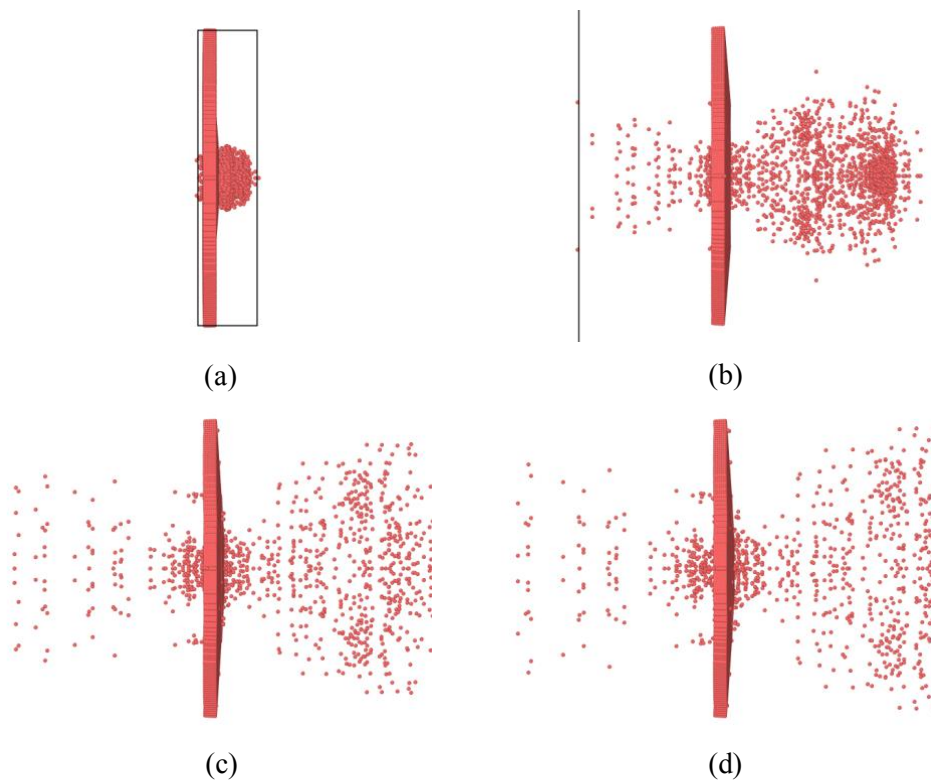


Fig. 7. Debris development at several simulation steps: (a) 200, (b) 800, (c) 1400, and (d) 1600 (velocity = 300 m/s, $\alpha = 0.25$, $k = 1E20$).

3.3. Influence of parameter

Observing the obtained simulation results, it can be said that while larger perforation and range of debris is produced with the increase of k value of indenter, the variation of parameter α seems to give somewhat different effects on the debris intensity. For lower k value, debris is observed to be more localized near the plate for greater α , as shown by Figs. 4 and 6. On the other hand, for higher value of k , debris is more localized near the plate for lower value of α ($\alpha = 0$), as depicted in Figs. 5 and 7.

Apart from that, nonetheless, consistent results are observed by increasing α value that the impacted plate appears to be more deflected. This observation can be seen by checking the shape of impacted plate at the final time step, as shown by Figs. 6 and 7, and Fig. 8 below.

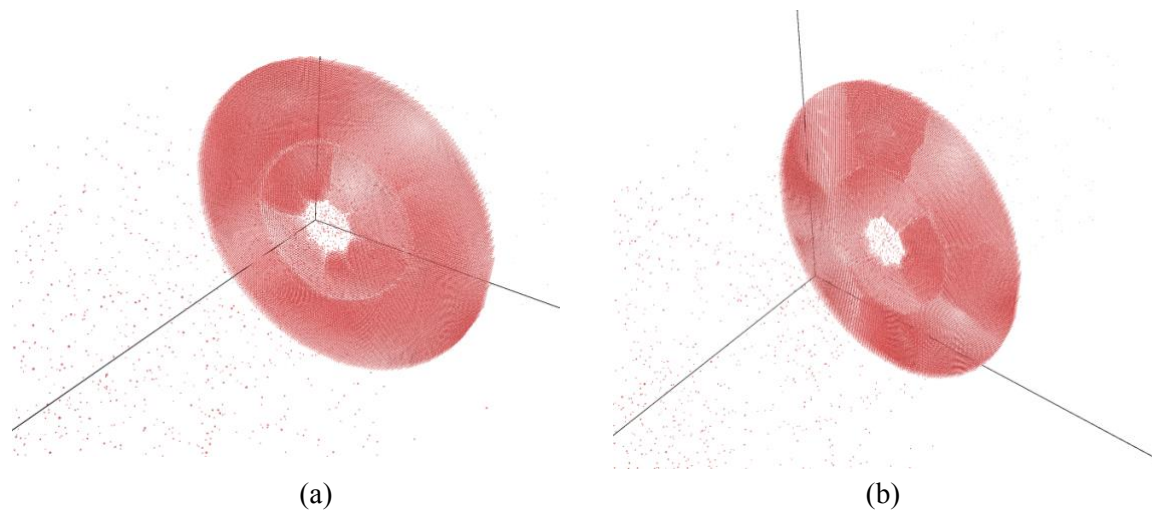


Fig. 8. Fracture surface and shape of the impacted plate at time step of 2000 for: (a) $\alpha = 0$, and (b) $\alpha = 0.25$ (velocity = 300 m/s and $k = 1E20$).

4. Conclusions

In this study, analysis of peridynamics has been presented for impact problems of projectile on aluminum target. Effects of indenter stiffness (k) and critical bond stretch parameter (α) on the produced perforation patterns are discussed for various impact velocities. Numerical results show that larger perforation is produced with the increase of k value of indenter. In addition, it is observed that the impacted plate appears to be more deflected, if greater value of α is employed. Evaluation of impact problems with different projectile characteristics would be subjects of future study.

5. Acknowledgements

This work was supported by the Penelitian Dana Lokal ITS Surabaya (No. 1325/PKS/ITS/2018) and partially funded by the Research Grant of PTUPT (128/SP2H/PTNBH/DRPM/2018) Ministry of Research, Technology and Higher Education of the Republic of Indonesia (Kemenristek DIKTI).

References

- [1] Reifsnider, K.L. ed., 1991. *Fatigue of Composite Materials*. Amsterdam: Elsevier.
- [2] Harris, B. ed., 2003. *Fatigue in Composites*. Cambridge: Woodhead Publishing Ltd.
- [3] Schijve, J. ed., 2009. *Fatigue of Structures and Materials*. Netherlands: Springer.

- [4] Griebel, M. and Schweitzer, M.A., 2000, “A particle partition of unity method for the solution of elliptic, parabolic, and hyperbolic PDEs”, *SIAM Journal of Scientific Computing*, 22, pp. 853–890.
- [5] Lucy, L.B. (1977), “A numerical approach to the testing of the fission hypothesis”, *Astron. J.*, Vol. 82, pp. 1013–24.
- [6] Gingold, R.A. and Monaghan, J.J. (1977), “Smoothed particle hydrodynamics: theory and application to non-spherical stars”, *Mon. Not. R. Astron. Soc.*, Vol. 181, pp. 375–89.
- [7] Atluri, S.N. and Shen, S.P. (2002), *The Meshless Local Petrov-Galerkin (MLPG) Method*, Tech Science Press, USA.
- [8] Liu, G.R. (2009), *Meshfree Methods: Moving Beyond the Finite Element Method*, 2nd ed., CRC Press, USA.
- [9] Parks, M.L., Seleson, P., Plimpton, S.J., Lehoucq, R.B. and Silling, S.A. (2010), *Peridynamics with LAMMPS: A User Guide v0.2 Beta*, SANDIA REPORT, Sandia National Laboratories, USA.
- [10] Silling, S.A. (2000), “Reformulation of elasticity theory for discontinuities and long-range forces”, *J. Mech. Phys. Solids*, Vol. 48(1), pp. 175–209.
- [11] Silling, S.A. and Askari, E. (2005), “A meshfree method based on the peridynamic model of solid mechanics”, *Comput. Struct.* Vol. 83(17), pp. 1526–35.
- [12] Bobaru, F., Yang, M., Alves, L.F., Silling, S.A., Askari, E. and Xu, J. (2009), “Convergence, adaptive refinement, and scaling in 1D peridynamics”, *Int. J. Numer. Meth. Engng.* Vol. 77(6), pp. 852–77.
- [13] Oterkus, S. and Madenci, E. (2012), “Peridynamic analysis of fiber-reinforced composite materials”, *J. Mech. Mater. Struct.* Vol. 7(1), pp. 45–84.
- [14] Stukowski, A. (2017), *OVITO User Manual*, Germany.
- [15] Mathworks (2013), *MATLAB User’s Guide (R2013a)*, USA.